JOURNAL OF PROPULSION AND POWER
Vol. 16, No. 5, September–October 2000

Design and Control of Solid-Fuel Ramjet for Pseudovacuum Trajectories

S. Krishnan,* Philmon George,† and S. Sathyan‡
Indian Institute of Technology Madras, Chennai 600 036, India

A ballistic trajectory in air of a powered projectile where the thrust always balances the drag is termed as a pseudovacuum trajectory. For a solid-fuel-ramjet (SFRJ)-powered gun-launched projectile this trajectory can be achieved by the control of engine mass-flow rate, either by a bypass control of inlet air or by a regression rate control of fuel. Based on one-dimensional considerations, the procedures for a preliminary design of the propulsion system for an SFRJ-assisted gun-launched projectile and the methods to calculate the control requirements are presented. Using these, typical configurations of SFRJ suitable for 155-mm gun-launched projectiles are analyzed for different launch angles. The results indicate that the control requirements by either method are minimal and thus, demonstrate the self-throttling characteristics of SFRJ.

Nomenclature

A	= constant in the regression-rate equation
A_e	= nozzle exit area
A_t	= nozzle throat area
D_{in}	= rearward step diameter
D_p	= initial fuel-grain-port diameter, mm
$D_{p,i}$	= instantaneous fuel-grain-port diameter, mm
D_t	= nozzle throat diameter
F	= thrust
G_a	= air mass flux through fuel grain port, kg/m^{2}s
L	= length of fuel grain
Mo_p	= molecular weight of combustion products
M_2	= Mach number at rearward step entry
$\dot{m}_{\text{ab}}$	= bypass air-mass-flow rate
$\dot{m}_{\text{ac}}$	= captured air-mass-flow rate
$\dot{m}_{\text{act}}$	= trial captured air-mass-flow rate under subcritical mode
$\dot{m}_{\text{as}}$	= off-design spillage air-mass-flow rate
$\dot{m}_{\text{at}}$	= trial air-mass-flow rate in the combustion chamber
$\dot{m}_b$	= mass-flow rate of combustion products
$\dot{m}_F$	= mass-flow rate of fuel
p_a	= atmospheric pressure
p_e	= nozzle-exit static pressure
p_{oa}, p_{o2}, p_{o3}, p_{o4}, p_{o5}, p_{o6}	= stagnation pressures at corresponding locations (Fig. 1)
p_{o2c}	= stagnation pressure at location 2 under critical mode
p'_{o5}	= stagnation pressure required to pass combustion gases through nozzle throat
p_3	= static pressure at port entry (location 3, Fig. 1), bar
Ru	= universal gas constant
$\dot{r}$	= fuel regression rate after control, mm/s
r_b	= combustion-chamber stagnation-pressure-loss factor, p_{o4}/p_{o3}
r_d	= operating stagnation-pressure-recovery ratio of inlet, p_{o2}/p_{oa}
r_{dc}	= critical stagnation-pressure-recovery ratio of inlet, p_{o2c}/p_{oa}
r_{no}	= nozzle stagnation-pressure-loss factor (overall), p_{o6}/p_{o4}
r_{nt}	= nozzle stagnation-pressure-loss factor (convergent portion), p_{o5}/p_{o4}
$\dot{r}_o$	= fuel regression rate, mm/s
r_r	= rearward-step stagnation-pressure-loss factor, p_{o3}/p_{o2}
$\dot{r}_t$	= fuel regression rate trial, mm/s
T_{oa}	= stagnation temperature of inlet air, K
T_{o4}	= stagnation temperature of combustion gases
T'_{o4}	= adiabatic flame temperature
T_3	= static temperature of air at port entry (location 3, Fig. 1), K
u	= projectile velocity
u_e	= nozzle-exit velocity
γ	= ratio of specific heats of combustion products
Δt	= time interval, s
η_b	= combustion efficiency, T_{o4}/T'_{o4}
Φ	= equivalence ratio

Introduction

THE velocity and range of a gun-launched projectile can be substantially increased by incorporating into it a propulsion system. Between the two possible propulsion systems, rocket and ramjet, the latter for the given total weight can provide higher range. Of the two ramjet types, namely the solid-fuel ramjet (SFRJ) and the liquid-fuel ramjet, the former represents a simpler design because of the absence of any moving part in its basic configuration. However, for control purposes the flight configuration of an SFRJ may contain certain moving components, but still it tends to be simpler than the liquid-fuel ramjet that uses a relatively complicated dynamic-feed system with associated controls. Quite a few research projects have been reported in the development of SFRJ-assisted gun-launched projectiles.[1–9]

The typical construction of an SFRJ-assisted gun-launched projectile is as given in Fig. 1. It has two parts. The front part has a diameter a little less than the gun barrel diameter for a loose fit, and this part houses a payload. At the nose of this front part is the inlet, closed by a frangible diaphragm. The rear part is of an outer diameter, which is considerably less than that of the front part and it forms the engine in which the fuel grain is stored. When in a gun barrel, a one-way valve inside the projectile (not shown in the figure), separating the front and the rear parts, together with an obturator on the periphery, serves as a piston.

The operating principle of an SFRJ-assisted gun-launched projectile is as follows. On firing, the gun-propellant combustion gases

Received 8 January 1998; revision received 31 March 1999; accepted for publication 13 August 1999. Copyright © 1999 by the American Institute of Aeronautics and Astronautics, Inc. All rights reserved.

*Professor and Head of Rockets and Missiles Laboratory, Department of Aerospace Engineering; skrish@aero.iitm.ernet.in. Associate Fellow AIAA.
†Ph.D. Research Scholar, Department of Aerospace Engineering.
‡B.Tech Student (Class of 1997), Department of Mechanical Engineering; currently Graduate Student, Department of Mechanical Engineering, University of Illinois at Urbana Champaign, Illinois 61801.

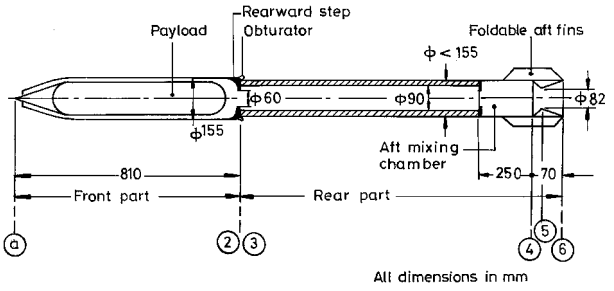

Fig. 1 SFRJ-assisted gun-launched projectile and reference locations.

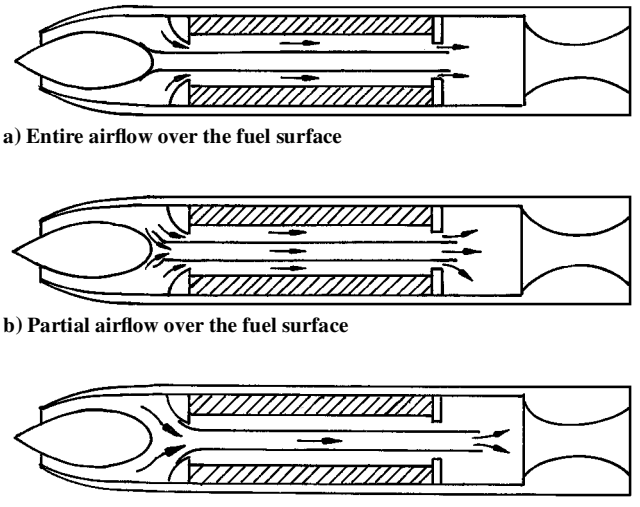

a) Entire airflow over the fuel surface

b) Partial airflow over the fuel surface

c) Least airflow over the fuel surface

Fig. 2 Tube-in-hole technique.

fill in the annular gap between the gun barrel and the rear part and the space within the engine (fuel grain port, aft mixing chamber, and nozzle passage). Forcing the piston, these high-pressure gases eject the projectile into the atmosphere at a supersonic Mach number of around two or more. The possibility of the fuel grain getting ignited within the gun barrel is precluded by two factors: 1) the travel time of the projectile within the gun barrel is of the order of a few milliseconds (< 10 ms) and 2) the gun propellant is mostly fuel rich. Now, the projectile having been ejected into the atmosphere, the opening of intake by the release of the frangible diaphragm and the gushing of air into the SFRJ take place in quick succession. Air flows in with a relatively high stagnation temperature of around 540 K or more. After external and internal deceleration processes, air enters the air inlet of the rearward step at a Mach number of around 0.3–0.4. Having been exposed to the high-temperature and very-high-pressure gases (a few thousand bars) within the gun barrel and now on being exposed to the high-temperature air, the surface of the fuel grain automatically gets ignited and releases combustion products. The hot combustion products thus released are accelerated through the nozzle with an exit momentum rate greater than the inlet value, thereby producing a thrust.

When an SFRJ flies at a lower altitude, as the air there is dense, it ingests large-air-mass-flow rate with high values of air mass flux, pressure, and temperature in the combustion chamber. The requirement of correspondingly high fuel flow rate for this large-air mass-flow rate can be met because the regression rate of fuel is proportional to air mass flux, pressure, and temperature. At higher altitudes, as the air there is thin, the SFRJ ingests low-air-mass-flow rate with reduced values of air-mass flux, pressure, and temperature in the combustion chamber. The requirement of correspondingly reduced fuel flow rate at this condition can be met because of the preceding regression-rate dependency. The self-throttling characteristics of SFRJ, thus, permit high-performance operation from sea-level to high-altitude conditions.

A pseudovacuum ballistic trajectory of a projectile in air is the one in which the drag experienced is always balanced by the thrust produced by the propulsive unit.[1] The adoption of this trajectory to an aerodynamically stable fire-and-forget projectile has two principal advantages, evidently in addition to the substantially enhanced velocity and range. The first one is the easy and accurate predictability of the trajectory. The second is the insensitiveness of the trajectory to external disturbances such as winds. Any crosswind will exert a force at the center of pressure of the projectile causing it to weathercock into the wind so that the resultant relative wind direction is in line with the projectile axis that subtends an angle to the original trajectory. The resulting enhanced drag (caused by the increase in the relative wind velocity) will be countered by an increased thrust from the propulsive unit maintaining the projectile on its original pseudovacuum trajectory. Head winds and tail winds will be similarly compensated by the thrust = drag control. To compensate any asymmetry, the projectile is usually given a spin (about 10% of a conventional projectile), and this results in a small computable drift of the trajectory.[2] Computational studies including transients with typical atmospheric profiles of real weather effects have shown that pseudovacuum ballistic trajectories under the thrust = drag control can be flown with a high precision leading to a circular error probable of even one order of magnitude less than that from an equivalent conventional trajectory (standard round or rocket assisted).[2,10] Among the options to achieve this trajectory, the SFRJ along with a sensitive accelerometer gives the simplest and, hence, the least-expensive solution. The accelerometer here senses any variation in axial acceleration and produces a signal that can monitor the engine mass-flow rate until the produced thrust balances the drag. Reference 2 presents further detailed discussion on the essential elements of an accelerometer control system for SFRJ in a gun-launched projectile. The control of engine mass-flow rate can be achieved either by a bypass control of inlet air or by a regression-rate control of fuel. In the first method a required quantity of inlet air is bypassed into the atmosphere without participating in combustion. For the projectile concept schematically given in Fig. 1, the bypass orifices can be located sufficiently upstream of the obturator such that it cannot block the bypass flow. This method of bypass control of inlet air is relatively a old one and is found adopted in many operating systems (for example, YF-12 aircraft and Concord use bypass control of inlet air).[11,12] In SFRJ this method was adopted in a 203-mm gun-launched projectile developed by Nordon Systems.[1] But, the second method is of recent origin and is specifically proposed for SFRJ and is known as the tube-in-hole technique.[13] A schematic arrangement of the tube-in-hole technique is shown in Fig. 2. In this, the regression-rate control of fuel is achieved by altering the effective air mass flux over the fuel surface using a translatory tube coaxially placed in the grain port hole. The tube splits the inlet airflow into two portions, one directed along the annular passage and the other through the center of the grain.

The present study, based on one-dimensional considerations, details procedures for a preliminary design of SFRJ for pseudovacuum trajectories. Also presented are the methods to calculate the control requirements for the bypass control of inlet air as well as the regression rate control of fuel. In this assessment exercise of the SFRJ sizing and the required thrust control, certain simplifying assumptions and procedures are used as detailed in the following:

1) The parameters are as follows: a) the launch angle is 30–45 deg, and b) the annular gap between the gun-barrel inner diameter and the projectile's rear-part outer diameter is 5–10 mm.

2) The gun ballistics are as follows: a) the kinetic energy of the projectile at launch is constant at 15.11 MJ, and b) the average length of fuel grain is used for the calculation of the combustion-chamber mass.

3) The drag calculations are as follows: a) zero angle of attack is assumed; b) the average length of fuel grain is used for the calculation of the total projectile length; c) wave drag is calculated through the semi-empirical relation by Miles (see Ref. 14) for an ogival nose of slenderness ratio = 2.5; d) friction drags for body and fins are calculated using the Karman–Shoenherr equation for compressible flow[14–16]; e) the interference drag is 5% of [c) + d)]; and f) the allowance for protuberances is 2% of [c) + d) + e)].

4) The inlet is as follows: a) the inlet diameter is infinitely variable; b) the critical stagnation-pressure recovery ratio of inlet is $r_{dc} = p_{o2c}/p_{oa} = f(M)$ (Ref. 17); and c) the flow is adiabatic.

5) The combustion chamber is as follows: a) the fuel-grain length is infinitely variable to give the stoichiometric fuel-air ratio; b) the wall thickness is 2.5 mm, and the material density is 8000 kg/m^3; c) the liner thickness is 2.5 mm, and the material density is 1000 kg/m^3; d) for better combustion efficiency an aft mixing combustion chamber is provided, and its length is 250 mm; e) the launch Mach number varies with respect to total mass of projectile, and this is typically around 2, with the maximum estimated inlet diameter as 55 mm and for $M_2 \leq 0.4$, D_{in} is fixed at 60 mm; f) for a stable-flammability condition D_p/D_{in} is 1.5, so that D_p is fixed at 90 mm; g) fuel density [polybutadiene:magnesium-aluminum alloy (50/50):nitroglycerine = 60:20:20] is 1150 kg/m^3; h) the fuel regression-rate is $\dot{r}_o = AG_a^{0.4} D_{pi}^{-0.25} T_{oa}^{0.4} p_3^{0.4}$ mm/s (A comes out as a solution), and the fuel-mass-flow rate is $\dot{m}_F = \pi D_{pi} L \dot{r}_o$; i) the adiabatic flame temperature, the ratio of specific heats, and the molecular weight of combustion products are calculated using a standard complex chemical equilibrium code such as CEC71 (Ref. 18); j) the combustion efficiency is $\eta_b = 0.9$; k) the rearward-step stagnation-pressure-loss factor is $r_r (\equiv p_{o3}/p_{o2}) = 0.95$; and l) the combustion-chamber stagnation-pressure-loss factor is $r_b (\equiv p_{o4}/p_{o3}) = 0.95$.

6) The nozzle is as follows: a) the nozzle throat is choked and infinitely variable; b) the adapted adiabatic nozzle expansion is assumed; c) the nozzle stagnation-pressure-loss factor (overall) is $r_{no} (\equiv p_{o6}/p_{o4}) = 0.9$; d) the nozzle stagnation-pressure-loss factor (convergent portion) is $r_{nt} (\equiv p_{o5}/p_{o4}) = 0.97$; and e) the nozzle length is 70 mm.

7) The thrust is shown with the following: Drag $= F = (\dot{m}_{ac} + \dot{m}_F) u_e - \dot{m}_{ac} u$.

For the two controls typical configurations of SFRJ suitable for 155-mm gun-launched projectiles are analyzed. The results indicate that the control requirements by either method are minimal and within practical limits.

Projectile Configurations

Certain basic SFRJ projectile configurations for the 155-mm gun have to be first estimated before starting the calculation of control requirements for a pseudovacuum trajectory. For this, based on a separate study the dimensions of major components except inlet diameter, fuel-grain length, and nozzle throat diameter were realized (Fig. 1). By the same study the mass of the projectile, except that of combustion chamber (comprising fuel grain, liner, and combustion-chamber shell), was estimated to be 51 kg. To complete the estimation of certain basic projectile configurations, a rubber-engine analysis was carried out as per the assumptions and procedures given in the preceding section. Rubber-engine analysis is one in which one or more of the engine components are assumed to be capable of infinite variability in configuration.[19] Here the inlet diameter, fuel-grain length, and nozzle throat diameter are assumed to be infinitely variable.

The projectile velocity at launch for the given gun and propellant charge depends on 1) the volume provided for the charge to burn, 2) the length of the projectile, and 3) the mass of the projectile. For the simplicity of analysis, the projectile velocity at launch was assumed to be dependent only on the mass of projectile for a constant kinetic energy of the projectile at launch.

Rearward-step stagnation-pressure-loss factor r_r and combustion-chamber stagnation-pressure-loss factor r_b can be calculated depending on the operating conditions at every instant.[20–22] As per the correlation found in Ref. 20, the value of r_r for the present configuration is found to decrease from 0.97 (at launch) to 0.95 (at touchdown). Similarly r_b is found to increase from 0.92 (at launch) to 0.96 (at touchdown).[22] In addition to these two factors, the sudden area variation from the grain port to aft mixing chamber will give a stagnation-pressure-loss factor changing from 0.95 (at launch) to 0.97 (at touchdown).[20] Generally the nozzle stagnation-pressure-loss factor is high, say 0.96–0.98. However, to maintain the simplicity of the procedure, in the present study except the inlet stagnation-pressure-recovery ratio r_{dc} all stagnation-pressure-loss factors are taken to be constant as given in the preceding section. The resulting gross-pressure-loss factor (excluding r_{dc}) of 0.81 (0.95 × 0.95 × 0.90) appears to be conservative because the worst situation that occurs at launch also works out to be 0.81 (0.97 × 0.92 × 0.95 × 0.96).

Combustion efficiency is dependent on several parameters including inlet air temperature and combustion-chamber pressure. With an increase in altitude, air temperature and combustion-chamber pressure will drop, and as a result η_b could reduce. At very high altitudes (>15,000 m) combustion may not be possible unless the combustion-chamber pressure is sufficiently high. In typical combustion-chamber configurations of SFRJ, combustion has been demonstrated at pressures above 0.5 bar, although the η_b is reported to be low at the limiting low pressure, around 0.7 (Ref. 21). Zvuloni et al. attained an average η_b above 0.93 for hydrocarbon fuels (HTPB, polymethylmethacrylate, and polyethylene) in the pressure and temperature ranges of 8–10 bar and 300–800 K, respectively.[23] For a nearly limiting high launch angle of 38 deg, the combustion chamber of the projectile configuration under study typically experiences a peak altitude <10,000 m, a pressure range of 1.5–6 bar, and a temperature range of 370–540 K. For lower launch angles the conditions are still more favorable. In view of the preceding, the assumption of an average $\eta_b = 0.9$ seems appropriate.

In the iterative scheme presented in the preceding section, the value of A in the fuel regression-rate equation comes out as a solution for the given launch angle and annular gap.

A typical result of the rubber-engine analysis, for launch angle of 35 deg and annular gap of 6.5 mm, is given in Fig. 3. From such results we note that for a given launch angle and annular gap 1) the fuel-grain length is maximum at touchdown, 2) the throat diameter is varying from the minimum at launch/touchdown to its maximum at peak altitude, and 3) the inlet diameter is varying from the maximum at launch/touchdown to its minimum at peak altitude.

For an actual engine to operate with a minimal bypass control of inlet air or regression-rate control of fuel, as the case may be, fixed values for fuel-grain length, throat diameter, and inlet diameter are to be carefully chosen. Although this choice is done more or less by trials—using the results of the rubber-engine analysis as the base—a general guideline however can be followed as per the following. First, regarding the fuel-grain length, an average value from rubber-engine results can be chosen. Nevertheless, this is treated as a parameter in the design analysis that is presented here. Second, regarding the choice of throat diameter, in order to pass the combustion products at all times let it be fixed for the moment at its maximum value Y (Fig. 3). Now the two control methods are to be considered separately for the choice of the third and the last quantity, namely, the inlet diameter. In the case of bypass control

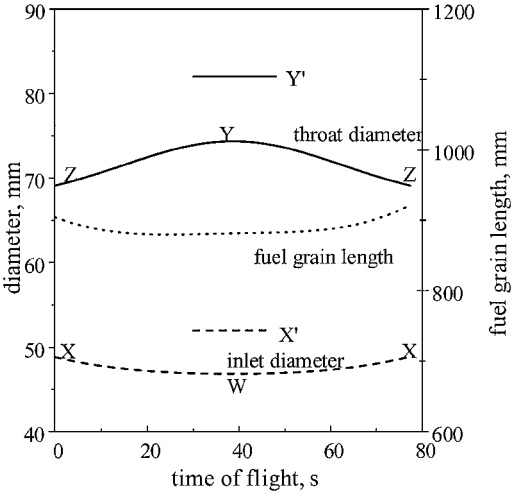

Fig. 3 Variation of fuel-grain length, throat diameter, and inlet diameter. The launch angle is 35 deg, the nose ogival slenderness ratio is 2.5, the annular gap is 6.5 mm, and the constant A in the regression-rate equation is 8.5×10^{-3}.

of inlet air, the chosen inlet diameter should have a value to ingest air mass-flow rates at all times. Therefore, it may seem at first sight that the inlet diameter may assume the value X (Fig. 3). But in practice the inlet diameter as well as the throat diameter have to be still higher than their respective X and Y values for the following reason. If the inlet diameter of X had been chosen, most significantly at touchdown condition the resulting (air + fuel) mass-flow rate has to pass through the throat of Y—fixed for the moment—instead of the corresponding smallest throat of Z (Fig. 3). Therefore, at this instant there should evidently be an enhanced stagnation-pressure loss that comes from a supercritical operation of the inlet. But with the resulting reduced pressure because of the supercritical operation p_3, the ingested air cannot generate the required fuel flow rate for thrust = drag condition (see regression-rate equation in the preceding section). Under the circumstances a mass-flow rate of air corresponding to the inlet diameter of X', higher than the one corresponding to X, should be ingested. This higher mass-flow rate of air along with the somewhat enhanced fuel flow rate (though not of stoichiometric but of fuel-lean value) gives thrust = drag requirement without bypass control of inlet air at touchdown. Thus, the chosen inlet diameter X' is always higher than X, and this difference $(X' - X)$ depends on the fuel-grain length. At other conditions, to realize thrust = drag requirement the tuning of the air mass-flow rate is necessary by bypassing a quantity of inlet air into the atmosphere without its participation in combustion. This bypassing cannot be to the extent of the rubber-engine base because the bypassed air in turn increases the total drag, demanding higher thrust than in the case of rubber engine. To achieve this demand, the engine mass-flow rate is augmented by a suitably retracted bypass that generates more $\dot{m}_F$. To negotiate such augmented mass-flow rates of engine at all times, most significantly at peak, the throat diameter has to be finally fixed at a value Y' even higher than Y. In the case of regression-rate control of fuel, because the control of total mass-flow rate comes through the control of fuel regression rate, the chosen inlet diameter for the actual engine can be less than X' (Fig. 3). However, this diameter is treated as a parameter in the analysis. Here again it can be argued to show that the throat diameter has to be fixed at a value higher than Y, as the inlet diameter is invariably chosen above X. In either of the control methods, however, D_t/D_p should be ≤ 0.91 for acceptable efficiency and stability of combustion.[24–26] Furthermore, this limiting value of 0.91 is acceptable only with high values of pressure and temperature that occur at launch. However after launch as the fuel regresses, the $D_t/D_{p,i}$ reduces giving acceptable lower values as the projectile ascends. Because D_p has already been fixed at 90 mm (see the preceding section), the maximum value that D_t can assume is 82 mm. In fact this maximum limit on D_t, as will be shown later, fixes the maximum possible launch angle for the projectile.

From the rubber-engine analysis with launch angles and annular gaps as parameters as per the preceding discussion, many trial engine configurations can be chosen. No detailed dimensional information is available on the configurations of operating SFRJs used for pseudovacuum trajectory projectiles. Nevertheless, the major dimensional ratios such as length-to-diameter ratio of engine or of whole projectile and mass per unit length of projectile of a typical trial configuration approximately match with those of a reported one.[1,24] Each of these trial configurations is characterized by an annular gap, a value of A, a fuel-grain length, a throat diameter, and an inlet diameter; and the configuration can be analyzed for the control requirements. The most suitable configuration is the one that can be operated closest to the stoichiometric condition for the widest range of launch angles, with the least control and the smallest sliver!

Control Requirements

The projectile is assumed to have an axisymmetric inlet with a center body of 45-deg cone angle. For the launch design Mach number, that is maximum, the diameter of the capture area is equal to the diameter of the chosen inlet area. But, for other lower Mach numbers the diameter of the capture area will be less, resulting in an off-design spillage[11,27] of $\dot{m}_{as}$ (caused by supercritical, critical, or subcritical mode), and this $\dot{m}_{as}$ is assumed to exit with zero axial momentum. Wind conditions affect projectile drag and inlet operation (air mass-flow rate, stagnation-pressure-recovery ratio, and supercritical margin), and the controls should be able to negotiate wind conditions and maintain the projectile on its pseudovacuum trajectory. Typical atmospheric profiles of real weather effects below tropopause generally indicate a maximum wind velocity of 15 m/s. For the projectile considered this will result in a sideslip angle—transient in nature—of less than 2 deg caused by side wind and the change in inlet air-mass-flow rate within 3% because of head/tail wind. Experimental results[28] on similar projectiles show negligible variation of drag coefficient for this change in slideslip angle in the Mach number range of 1–2; the projectile operates in the Mach-number range of 1.7–2 and below tropopause. The change in inlet operating conditions because of wind conditions tends to reduce the maximum launch angle capability and demand wind conditions dependent controls. These can be calculated by a simple extension to the present basic procedure that is given for a no-wind condition.

Bypass Control of Inlet Air

In this method the control is possible only when the inlet is operating under critical or supercritical mode. As per the preceding discussion, to negotiate the launch/touchdown condition the chosen inlet diameter is higher than the maximum value from rubber-engine analysis. With this higher value of inlet diameter, most of the time the captured air mass-flow rate $\dot{m}_{ac}$ and the resulting fuel flow rate are unsuitable for the condition of pseudovacuum trajectory. Therefore, the tuning of the combustor air-mass-flow rate is done by bypassing $\dot{m}_{ab}$ from the captured air-mass-flow rate $\dot{m}_{ac}$. For a conservative estimate $\dot{m}_{ab}$ is also assumed to exit with zero axial momentum. With all of these, for a chosen trial configuration the control characteristics can be calculated for various launch angles as per the following procedure:

Step I: At an arbitrary time, using the flight velocity and atmospheric conditions calculate p_{oa}, p_{o2}, p_{o4}, p_{o5}, p_{o6}, T_{oa}, p_3, T_3, and the total drag (Introduction section).

Step II: Calculate the captured air-mass-flow rate $\dot{m}_{ac}$ after accounting for off-design spillage $\dot{m}_{as}$ (Refs. 11 and 27).

Step III: Choose a trial air-mass-flow rate in the combustion chamber $\dot{m}_{at}$. Evidently $\dot{m}_{at} \leq \dot{m}_{ac}$; $\dot{m}_{ab} = (\dot{m}_{ac} - \dot{m}_{at})$ is bypassed.

Step IV: Calculate the fuel regression rate (Introduction section) and hence $\dot{m}_F$.

Step V: Calculate adiabatic flame temperature T'_{o4}, γ, and Mo_p using CEC71 with the preceding ratio of $\dot{m}_{at}$ and $\dot{m}_F$ and p_3. Calculate T_{o4} using η_b.

Step VI: Calculate u_e, p_e, and hence the thrust,

$$F = (\dot{m}_{at} + \dot{m}_F)u_e - (\dot{m}_{ac} + \dot{m}_{as})u + (p_e - p_a)A_e \qquad (1)$$

Step VII: Check whether this thrust is equal to the drag. If not, go to step III.

Step VIII: Calculate the nozzle throat stagnation pressure p'_{o5} required to pass the mass-flow rate of combustion products $\dot{m}_b = (\dot{m}_{at} + \dot{m}_F)$:

$$p'_{o5} = \frac{\dot{m}_b \sqrt{RuT_{o4}/Mo_p}}{A_t \sqrt{\gamma}(2/\gamma + 1)^{\{\gamma + 1/2(\gamma - 1)\}}} \qquad (2)$$

Step IX: Check whether $p'_{o5} \leq p_{o5}$. If $p'_{o5} < p_{o5}$, the inlet is operating in supercritical mode (operating $p_{o2}/p_{oa} < r_{dc}$); set p_{o5} equal to p'_{o5}; recalculate p_{o4}, p_{o6}, p_{o3}, and operating p_{o2} using r_{nt}, r_{no}, r_b, and r_r respectively; and go to step IV. If $p'_{o5} > p_{o5}$, the inlet is operating in subcritical mode, and bypass control is no longer effective. Hence abort the calculations. If $p'_{o5} = p_{o5}$, then the prior $\dot{m}_{ab}$ is the one to be bypassed.

Step X: Under quasi-steady-state assumption, calculate the new port diameter after the time interval Δt:

$$D_{p,i+1} = D_{p,i} + 2\dot{r}_i \Delta t \qquad (3)$$

Go to Step I with the new temporal and spatial values until the total time of flight is covered.

Regression-Rate Control of Fuel

Here as for the preceding case is chosen a trial configuration, characterized by an annular gap, a value of A, a fuel-grain length, a throat diameter, and an inlet diameter. Contrary to the preceding control method, the entire captured air mass flow participates in combustion, and the necessary balancing of thrust with drag is obtained by adjusting the fuel regression rate from $\dot{r}_o$ (the regression rate corresponding to the unaltered air-mass flux in grain port) to $\dot{r}$ (the one corresponding to the altered air-mass flux in the grain port because of splitting). The control characteristics can be calculated for various launch angles as per the following procedure.

Step I: At an arbitrary time using the flight velocity and atmospheric conditions, calculate p_{oa}, p_{o2}, p_{o4}, p_{o5}, p_{o6}, T_{oa}, p_3, T_3, and the total drag (Introduction section).

Step II: Calculate the captured air-mass-flow rate $\dot{m}_{ac}$ after accounting for off-design spillage.

Step III: Choose a trial fuel regression rate $\dot{r}_t$, and calculate the fuel-mass-flow rate $\dot{m}_F$.

Step IV: Calculate adiabatic flame temperature T'_{o4}, γ, and Mo_p using CEC71 with the preceding ratio of $\dot{m}_{ac}$ and $\dot{m}_F$ and p_3. Calculate T_{o4} using η_b.

Step V: Calculate u_e, p_e, and hence the thrust

$$F = (\dot{m}_{ac} + \dot{m}_F)u_e - (\dot{m}_{ac} + \dot{m}_{as})u + (p_e - p_a)A_e \qquad (4)$$

Step VI: Check whether this thrust is equal to the drag. If not, go to step III.

Step VII: Calculate the nozzle throat stagnation pressure p'_{o5} required to pass the mass-flow rate of combustion products $\dot{m}_b = (\dot{m}_{ac} + \dot{m}_F)$ using Eq. (2).

Step VIII: Check whether $p'_{o5} \leq p_{o5}$. If $p'_{o5} < p_{o5}$, the inlet is operating in supercritical mode (operating $p_{o2}/p_{oa} < r_{dc}$); set p_{o5} equal to p'_{o5}; recalculate p_{o4}, p_{o6}, p_{o3}, and operating p_{o2} using r_{nt}, r_{no}, r_b, and r_r respectively; and go to step IV. If $p'_{o5} > p_{o5}$ (the inlet is operating in subcritical mode and subcritical off-design spillage will occur), go to step XI.

Step IX: Calculate the regression rate $\dot{r}_o$ using the regression-rate equation (Introduction section) for $\dot{m}_{ac}$ and p_3 and the regression rate ratio $\dot{r}_t/\dot{r}_o$.

Step X: Under quasi-steady-state assumption calculate the new port diameter after the time interval Δt using Eq. (3). Go to Step I with the new temporal and spatial values until the total time of flight is covered.

Step XI: Choose a trial captured air-mass-flow rate $\dot{m}_{act}$. Evidently $\dot{m}_{act} \leq \dot{m}_{ac}$; $(\dot{m}_{ac} - \dot{m}_{act})$ is the subcritical spillage mass-flow rate.

Step XII: Calculate the adiabatic flame temperature T'_{o4}, γ, and Mo_p using CEC71 with the ratio of $\dot{m}_{act}$ and $\dot{m}_F$. Calculate T_{o4} using η_b.

Step XIII: Calculate the nozzle stagnation pressure p'_{o5} required to pass the mass-flow rate of combustion products $\dot{m}_b = (\dot{m}_{act} + \dot{m}_F)$ using Eq. (2). If $p'_{o5} \neq p_{o5}$, go to step XI.

Step XIV: Calculate u_e, p_e, and hence the thrust

$$F = (\dot{m}_{act} + \dot{m}_F)u_e - (\dot{m}_{ac} + \dot{m}_{as})u + (p_e - p_a)A_e \qquad (5)$$

Step XV: Check whether this thrust is equal to the drag. If yes, set $\dot{m}_{ac} = \dot{m}_{act}$ and go to step IX. If not, choose a new trial regression rate $\dot{r}_t$ and hence new trial fuel-mass-flow rate $\dot{m}_F$ and go to step XII.

Results and Discussion

Several trial engine configurations each characterized by an annular gap, a value of A, a fuel-grain length, a throat diameter, and an inlet diameter were analyzed for the control requirements for the range of launch-angle capability from 30 to 45 deg (Ref. 29). This analysis indicates that the lower launch angle (because of higher drag) demands larger quantity of fuel (smaller annular gap). Also it points out that the wider range of launch angles can be achieved with a larger value of throat diameter D_t. Now for the presentation of other control characteristics, we have to choose a fixed engine configuration and a fuel type. An annular gap of 6.5 mm is chosen for the engine with bypass control of inlet air. This gap for the engine with regression-rate control of fuel is taken as 5.5 mm. Based on the results of the analysis for different launch angles and annular gaps and also taking into consideration the typical regression-rate values reported in the literature for HTPB fuel,[22,30] a value of 8.5×10^{-3} is assigned to A. The maximum possible value of 82 mm is used for D_t in order to have a wider range of launch angles. The other two, fuel-grain length and inlet diameter, are taken as parameters for the analysis. However, for the bypass control of inlet air, given the value of fuel-grain length and zero bypass ratio at touchdown, the inlet diameter comes out as a solution.

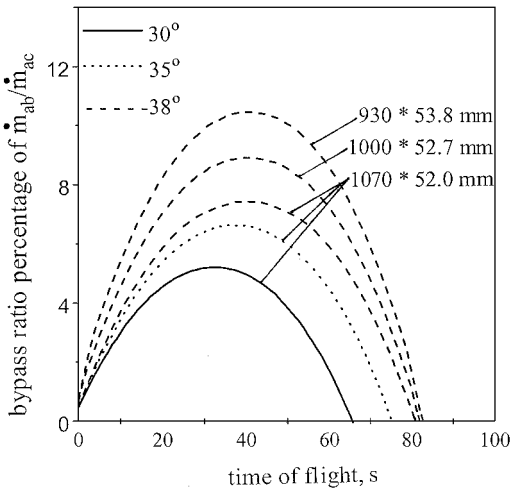

Fig. 4 Percentage variations of bypass ratio of inlet air. The nose ogival slenderness ratio is 2.5, the annular gap is 6.5 mm, the constant A in the regression-rate equation is 8.5×10^{-3}, and the throat diameter is 82 mm.

Bypass Control of Inlet Air

The percentage variations of bypass ratio for three different fuel-grain lengths and their corresponding inlet diameters are shown in Fig. 4. Also shown are the percentage variations of the same at a fuel-grain length of 1070 mm for launch angles of 30, 35, and 38 deg. With the increase in grain length and the corresponding decrease in inlet diameter, the contribution of $\dot{m}_F$ to the total mass-flow rate of combustion products $\dot{m}_b$ $(= \dot{m}_{ac} - \dot{m}_{ab} + \dot{m}_F)$ increases; therefore, the requirement of bypass control on inlet air decreases. But with the increase in launch angle because the projectile is required to operate at higher altitudes (wider environmental changes), the maximum bypass control requirement increases. For a projectile of a given configuration, the limitation on maximum launch angle comes because of the inability of the chosen throat to pass the required $\dot{m}_b$ $(p'_{o5} > p_{o5})$. The way to remove this limitation lies in the increase of throat diameter, but with the constraint of $D_t/D_p \leq 0.91$ for the chosen D_p the maximum possible $D_t = 0.91 \times D_p$, as already indicated. Any further increase in D_t is possible only with the corresponding increase in D_p. Here, for the specified annular gap this increase in D_p will in turn need a longer grain with an unrealistically slow fuel regression rate.

The equivalence ratio Φ is the ratio of the operating fuel/air ratio to the stoichiometric fuel/air ratio. The variations of Φ for three different grain lengths are shown in Fig. 5. Also shown are the variations of Φ at a fuel-grain length of 1070 mm for launch angles of 30, 35, and 38 deg. The variation of grain length affects Φ, and as expected the longer length can shift the engine operation to the fuel-rich side. By choosing an appropriate grain length, the engine can be made to operate near the desired equivalence ratio.

In this method of bypass control of inlet air because the inlet can operate in supercritical or critical mode, the enhanced stagnation-pressure loss because of supercritical operation is of interest. This can be characterized by r_d/r_{dc}, where r_d $(= p_{o2}/p_{oa})$ is the operating stagnation-pressure-recovery ratio of inlet. Shown in Fig. 6 are the variations of r_d/r_{dc} at a fuel-grain length of 1070 mm for launch angles of 30, 35, and 38 deg. At a peak altitude as the actual engine

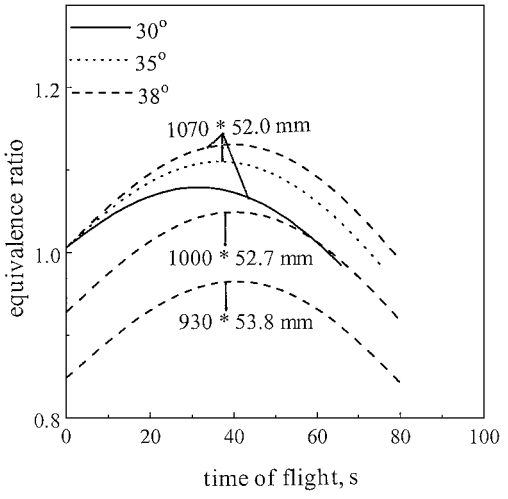

Fig. 5 Equivalence-ratio variations under bypass control of inlet air. The nose ogival slenderness ratio is 2.5, the annular gap is 6.5 mm, constant A in the regression-rate equation is 8.5×10^{-3}, and the throat diameter is 82 mm.

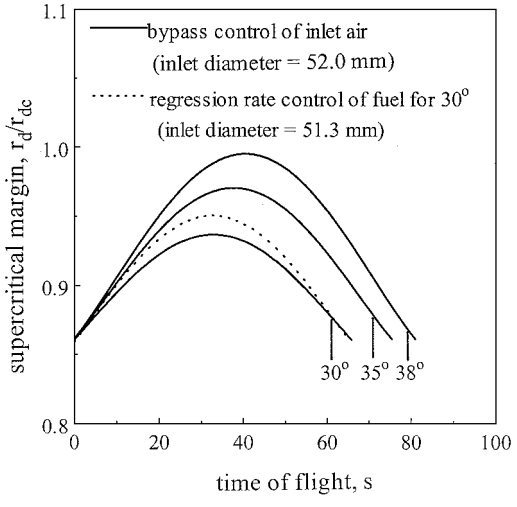

Fig. 6 Inlet operation under bypass control of inlet air and regression-rate control of fuel. The fuel-grain length is 1070 mm, the nose ogival slenderness ratio is 2.5, the annular gap is 6.5 mm, the constant A in the regression-rate equation is 8.5×10^{-3}, and the throat diameter is 82 mm.

has its throat diameter closest to the one of the rubber engine (Fig. 3), the r_d / r_{dc} is at its maximum.

A representative regression-rate variation in flight according to the assumed equation is shown in Fig. 7. The corresponding trajectory profile is also given. To demonstrate the wide variation in operating conditions, a high launch angle of 38 deg is chosen. The experimental regression rates reported in literature for HTPB fuel are also marked in the figure. Reference 22 gives an experimental correlation for an HTPB fuel. Using this correlation, for typical flight conditions the regression rates were calculated and are presented. However, in Ref. 30 the experiments were conducted for an HTPB fuel at a lower D_p of 10 mm and a relatively higher constant stagnation temperature of 540 K. These experimental data indicate that the assumed regression-rate equation is representative of a typical HTPB fuel.

Regression-Rate Control of Fuel

In this method, although the inlet can operate under subcritical mode and still deliver thrust = drag condition, the required variation of regression-rate ratio is sharp and large once the inlet enters into subcritical mode as shown in Fig. 8. Such a sharp variation may not

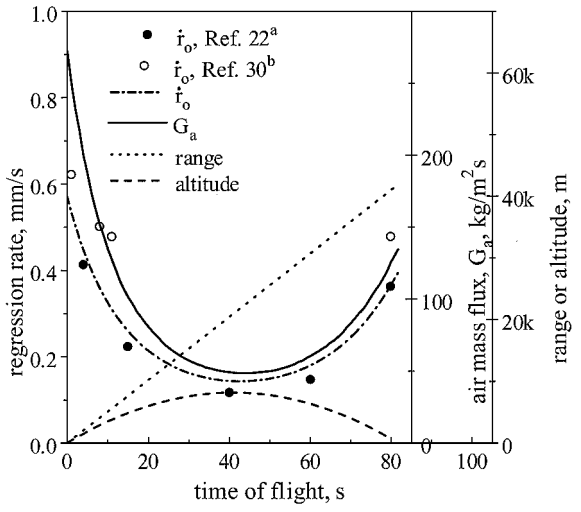

Fig. 7 Variations of range, altitude, regression rate, and air-mass flux with time of flight. The launch angle is 38 deg, the fuel-grain length is 1000 mm, the inlet diameter is 52.0 mm, the nose ogival slenderness ratio is 2.5, the annular gap is 6.5 mm, the constant A in the regression-rate equation is 8.5×10^{-3}, and the throat diameter is 82 mm. [a]Regression rate is calculated using experimental correlation of Ref. 22 for identical values of air-mass flux, inlet stagnation temperature, and static pressure. [b]Test data of Ref. 30 for D_p = 10 mm and T_{oa} = 540 K.

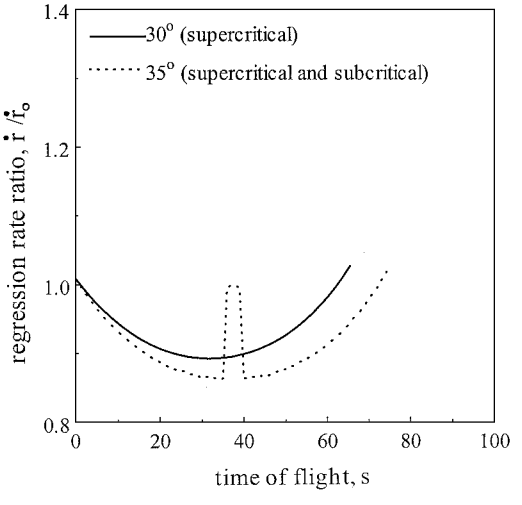

Fig. 8 Regression-rate ratio variations for supercritical and subcritical operations. The fuel-grain length is 1070 mm, the inlet diameter is 52.0 mm, the nose ogival slenderness ratio is 2.5, the annular gap is 5.5 mm, the constant A in the regression-rate equation is 8.5×10^{-3}, and the throat diameter is 82 mm.

be possible by a control system. Therefore the results of subcritical modes of operations are not presented here.

The variations of regression-rate ratio for three different inlet diameters are shown in Fig. 9. Also shown are the variations of the same at an inlet diameter of 50.5 mm for launch angles of 30, 35, and 38 deg. For a given launch angle with the increase in inlet diameter and the corresponding increase in captured air-mass-flow rate $\dot{m}_{ac}$, the regression rate $\dot{r}_o$ is high. But relative to $\dot{m}_{ac}$, to satisfy thrust = drag condition the required fuel-flow rate is less and so also the required regression rate. Consequently, the regression-rate ratio $\dot{r}/\dot{r}_o$ decreases with the increase in inlet diameter. For given inlet diameter and launch angle the regression-rate ratio decreases from launch to a minimum at peak and then increases to its maximum at touchdown. This behavior can be argued to be caused by 1) the chosen inlet diameter being less than X' but higher than W (see Fig. 3) and 2) the r_d / r_{dc}, coming from supercritical operation, being lowest at launch/touchdown (see Fig. 6). To estimate the load on the

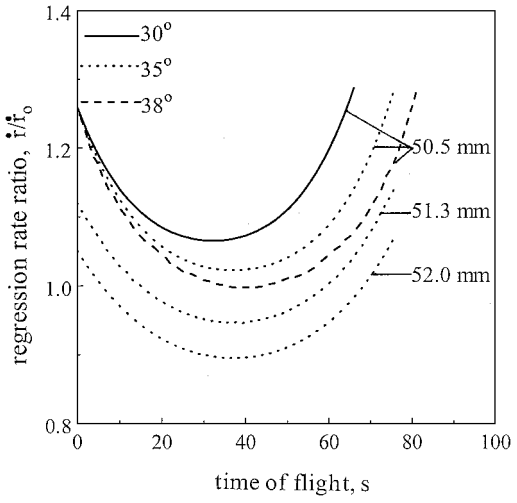

Fig. 9 Regression-rate ratio variations under regression-rate control of fuel for different inlet diameters. The fuel-grain length is 1000 mm, the nose ogival slenderness ratio is 2.5, the annular gap is 5.5 mm, the constant A in the regression-rate equation is 8.5×10^{-3}, and the throat diameter is 82 mm.

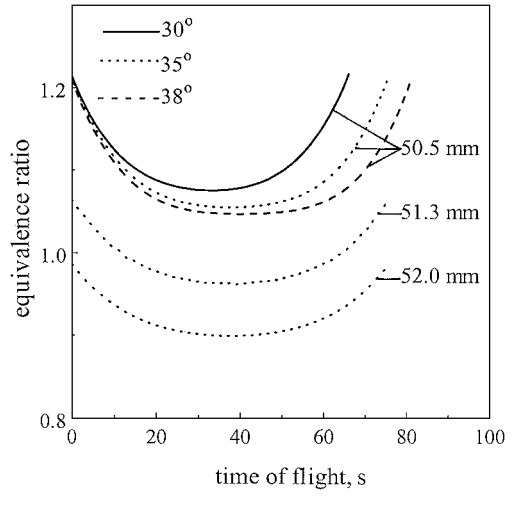

Fig. 10 Equivalence-ratio variations under regression-rate control of fuel for different inlet diameters. The fuel-grain length is 1000 mm, the nose ogival slenderness ratio is 2.5, the annular gap is 5.5 mm, the constant A in the regression-rate equation is 8.5×10^{-3}, and the throat diameter is 82 mm.

control system, it is of interest to consider the ratio of the preceding maximum and the minimum. If we designate this as control ratio, it is found to decrease with the increase in inlet diameter; however, this variation is very small.

The variations of Φ for three different inlet diameters are shown in Fig. 10. Also shown are the variations of Φ at an inlet diameter of 50.5 mm for launch angles of 30, 35, and 38 deg. The variation of inlet diameter affects the Φ, and as expected the smaller inlet can shift the engine operation to the fuel-rich side. By choosing an appropriate inlet diameter, the engine can be made to operate near the desired equivalence ratio.

Under regression-rate control of fuel, among the chosen inlet diameters the lowest inlet diameter is found to provide the highest launch-angle capability to the projectile. The reason for this can be explained as follows. From rubber-engine analysis one can see that at peak the throat diameter is maximum and the inlet diameter is minimum (Fig. 3). These extrema further increase and decrease respectively with increase in launch angles. For the actual engine the throat diameter is fixed above this maximum as per the preceding discussion (of course with the limit $D_t/D_p = 0.91$). At peak, furthermore, an inlet diameter fixed closer to the preceding minimum

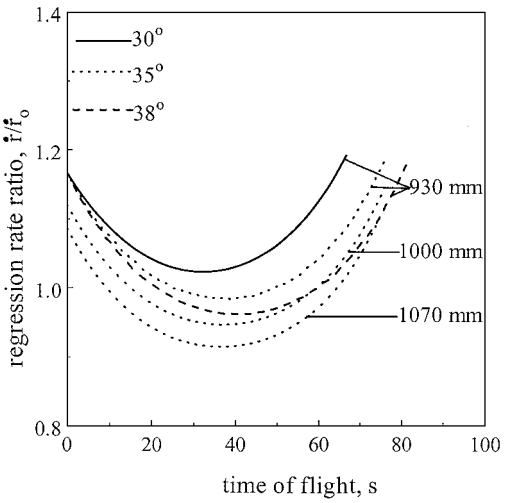

Fig. 11 Regression-rate ratio variations for different fuel lengths. The inlet diameter is 51.3 mm, nose ogival slenderness ratio is 2.5, the annular gap is 5.5 mm, the constant A in the regression-rate equation is 8.5×10^{-3}, and the throat diameter is 82 mm.

keeps the excess air flowing into the actual engine less. Therefore, the lower the inlet diameter the higher is the launch-angle capability. But this higher launch angle capability is achieved sometimes sacrificing the lower launch-angle operation for the given annular gap. For example with 930-mm fuel-grain length and annular gap of 5.5 mm, lowering the inlet diameter from 52 to 50.5 mm increases the higher launch-angle capability from 38 to 40 deg; but 52-mm inlet diameter can work at a 30-deg launch angle, whereas a 50.5-mm one cannot because of the inadequacy of fuel.

The variations of regression-rate ratio for three different fuel-grain lengths are shown in Fig. 11. Also shown are the variations of the same at a fuel-grain length of 930 mm for launch angles of 30, 35, and 38 deg. For a given inlet diameter and air-mass flux the fuel-mass-flow rate increases with the increase in fuel-grain length. Therefore the mean regression-rate-ratio requirement decreases with the increase in fuel-grain length. The control ratio decreases with the decrease in fuel-grain length; however, this variation is very small.

In the method of regression-rate control of fuel, among the chosen fuel-grain lengths, the shortest fuel-grain length provides the highest launch-angle capability to the projectile. The principal reason for this is that the drag of the projectile decreases with the reduction in fuel-grain length. But this higher launch-angle capability is achieved sometimes sacrificing the lower launch-angle operation for the given annular gap. For example with 50.5-mm inlet diameter and annular gap of 5.5 mm, lowering the fuel-grain length from 1070 to 930 mm increases the higher launch-angle capability from 37 to 40 deg, but 1070-mm fuel-grain length can work at a 30-deg launch angle, whereas a 930-mm one cannot because of the inadequacy of fuel.

A typical curve of r_d/r_{dc} in the regression-rate control of fuel is also shown in Fig. 6. The variations are similar to the ones in bypass control of inlet air.

Maximum Launch-Angle Capability

Using the preceding two calculation procedures, maximum launch-angle capability of a projectile configuration can be calculated. The higher the launch angle the higher is the range, but the wider are the environmental changes. The limit on the maximum launch angle comes because of the inlet operating at critical condition at the corresponding peak altitude. Most ramjet systems are operated with a comfortable margin away from this critical condition because many inlet designs including annular ones have no subcritical operating region. If such an inlet is operated at or near its critical condition, then it is very easy to drive the inlet directly into its buzz condition. When this happens, combustion blowout is imminent. Furthermore, as explained earlier either of the two controls cannot be operated under subcritical mode. Therefore a supercritical margin

for operation must be used and be based on a total knowledge of all geometries, engine pressure losses, and combustion characteristics. When these parameters are assumed from general literature, a safe supercritical margin of at least 5% may have to be assumed to fix the maximum launch-angle capability.

Conclusions

For an SFRJ-assisted projectile to operate under a pseudovacuum trajectory with a minimal bypass control of inlet air or regression-rate control of fuel, a set of fixed dimensions of fuel-grain length, throat diameter, and inlet diameter can be chosen from rubber-engine analysis. This choice gives the preliminary design configuration for the engine.

In the method of bypass control of inlet air, the choice of fuel-grain length correspondingly fixes the inlet diameter. In this method the control requirements decrease with the increase in fuel-grain length. The mean operating fuel/air ratio increases with the increase in fuel-grain length. Hence, by choosing an appropriate grain length, the engine can be made to operate near the desired fuel/air ratio condition.

In the method of regression-rate control of fuel, the required variation of regression-rate ratio is sharp and large once the inlet enters into subcritical mode. Hence this control under subcritical mode appears to be very difficult to be realized. Lower inlet diameter or shorter fuel-grain length is found to provide higher launch-angle capability to the projectile. The mean operating fuel/air ratio increases with the decrease in inlet diameter and/or the increase in fuel-grain length. By choosing an appropriate inlet diameter or fuel-grain length, the engine can be made to operate near the desired fuel/air ratio condition.

Acknowledgment

S. Santhakumar, Professor of Aerospace Engineering of the Indian Institute of Technology Madras, actively participated in many discussions concerning the aerodynamic and control aspects of the present study.

References

[1]Fink, M. R., "Aerodynamic Properties of an Advanced Indirect Fire System (AIFS) Projectiles," *Journal of Spacecraft and Rockets*, Vol. 19, No. 1, 1982, pp. 36–40.

[2]Simpson, J. A., "Flight Dynamics of the Advanced Fire System (AIFS)—Cannon Launched Ramjet," *Proceedings of 7th International Symposium on Ballistics*, American Defense Preparedness Association, Arlington, VA, 1983, pp. 455–462.

[3]Simpson, J. A., Krier, H., and Butler, P. B., "Interior Ballistics for Launch Dynamics for Advanced Indirect Fire System," *Proceedings of 7th International Symposium on Ballistics*, American Defense Preparedness Association, Arlington, VA, 1983, pp. 445–453.

[4]Gany, A., "Analysis of Gun-Launched, Solid Fuel Ramjet Projectiles," *Base Bleed: Proceedings of the First International Symposium on Special Topics in Chemical Propulsion*, edited by K. K. Kuo and J. N. Fleming, Hemisphere, Washington, DC, 1991, pp. 289–309.

[5]Nusca, M. J., Chakravarthy, S. R., and Goldberg, U. C., "Computational Fluid Dynamics Capability for Solid Fuel Ramjet Projectile," *Journal of Propulsion and Power*, Vol. 6, No. 3, 1990, pp. 256–262.

[6]Nusca, M. J., "Steady Flow Combustion Model for Solid Fuel Ramjet Projectile," *Journal of Propulsion and Power*, Vol. 6, No. 3, 1990, pp. 348–352.

[7]Veraar, R. G., "Ramjet Applications of the Solid Fuel Combustion Chamber," *Proceedings of Symposium on the Solid Fuel Combustion Chamber and Beyond*, 1991, pp. 129–146.

[8]Wimmerstrom, P., Nilsson, Y., and Gunners, N. E., "Initial Study of a 40 mm SFRJ Projectile," *Proceedings of 14th International Symposium on Ballistics*, Vol. 1, edited by M. J. Murphy and J. E. Backofen, American Defense Preparedness Association, Arlington, VA, Sept. 1993, pp. 721–733.

[9]Ivarsson, U., "Entirely up to Speed," *International Defense Review*, March 1994, p. 63.

[10]Santhakumar, S., Madhavan, A., and Vijay, K. N., "Trajectory Simulation of a Thrust Controlled, SFRJ Propelled, Cannon Launched Projectile," *Journal of the Aeronautical Society of India*, Vol. 50, No. 2, 1998, pp. 93–99.

[11]Mahoney, J. J., *Inlets for Supersonic Missiles*, AIAA Education Series, AIAA, Washington, DC, 1991, pp. 115–118, 185–187.

[12]"Refinement on Inlet Design Continues," *Aviation Week and Space Technology*, Vol. 94, No. 6, 1971, pp. 62–64.

[13]Keirsey, J. L., "Solid Fuel Ramjet Flow Control Device," United States Patent 628 688, Dec. 1986.

[14]Chin, S. S., *Missile Configuration Design*, McGraw–Hill, New York, 1961, pp. 23–25, 64–67.

[15]Locke, F. W. S., Jr., "Recommended Definition of Turbulent Friction in Incompressible Fluids," Bureau of Aeronautics Research Div. Rept. 1415, June 1952.

[16]Rubesin, M. W., Maydew, R. C., and Varga, S. A., "An Analytical and Experimental Investigation of the Skin Friction of the Turbulent Boundary Layer on a Flat Plate at Supersonic Speeds," NACA TN-2305, Feb. 1951.

[17]Mattingly, J. D., Heiser, W. H., and Daley, D. H., *Aircraft Engine Design*, AIAA Education Series, AIAA, Washington, DC, 1987, pp. 106, 107.

[18]Gordon, S., and McBride, B. J., "Computer Program for Calculation of Complex Chemical Equilibrium Compositions, Rocket Performance, Incident and Reflected Shocks, and Chapman-Jouguet Detonations," NASA SP-273, March 1976.

[19]Kerrebrock, J. L., *Aircraft Engines and Gas Turbines*, MIT Press, Cambridge, MA, 1987, p. 21.

[20]Vonderwell, D. J., Murray, I. F., and Heister, S. D., "Optimization of Hybrid-Rocket-Booster Fuel-Grain Design," *Journal of Spacecraft and Rockets*, Vol. 32, No. 4, 1990, pp. 964–969.

[21]Myers, T. D., "Special Problems of Ramjet with Solid Fuel," *Ramjet and Ramrocket Propulsion Systems for Missiles*, AGARD PEP Lecture Series 136, Sept. 1984.

[22]Leisch, S., and Netzer, D. W., "Solid Fuel Ramjets," *Tactical Missile Propulsion*, edited by G. E. Jenson and D. W. Netzer, Vol. 170, Progress in Astronautics and Aeronautics, AIAA, Washington, DC, 1996, pp. 469–496.

[23]Zvuloni, R., Levy, Y., and Gany, A., "Investigation of a Small Solid Fuel Ramjet Combustor," *Journal of Propulsion and Power*, Vol. 5, No. 3, 1989, pp. 269–275.

[24]"Solid Fuel Ramjet," United Technologies Chemical Systems, San Jose, CA, 1980.

[25]Netzer, A., and Gany, A., "Burning and Flameholding Characteristics of a Miniature Solid Fuel Ramjet Combustor," *Journal of Propulsion and Power*, Vol. 7, No. 3, 1991, pp. 357–363.

[26]Wooldridge, R. C., and Netzer, D. W., "Ignition and Flammability Characteristics of Solid Fuel Ramjets," *Journal of Propulsion and Power*, Vol. 1, No. 5, 1991, pp. 846–848.

[27]Anderson, J. D., *Modern Compressible Flow with Historical Perspective*, McGraw–Hill, New York, 1990, pp. 294–306.

[28]Dahlke, C. W., and Flowers, L. D., "The Aerodynamic Characteristics of Wrap-Around Fins, Including Fold Angle at Mach Numbers from 0.5 to 3.0," U.S. Army Missile Command, RD-75-15, Redstone Arsenal, AL, Nov. 1974.

[29]Philmon, G., "Solid Fuel Regression Rate Studies in Hybrid Rockets and Solid Fuel Ramjets," Ph.D. Dissertation, Dept. of Aerospace Engineering, Indian Inst. of Technology Madras, Chennai, India, June 1998.

[30]Harder, I., and Gany, A., "Fuel Regression Rate Mechanism in a Solid Fuel Ramjet," *Propellants, Explosives, and Pyrotechnics*, Vol. 17, No. 3, 1992, pp. 70–76.